Full paper/Mémoire

Modulation of the unpaired spin localization in Pentavalent Uranyl Complexes

Valentina Vetere [a,b], Pascale Maldivi [a,*], Marinella Mazzanti [a]

[a] INAC, SCIB, laboratoire de reconnaissance ionique et chimie de coordination, CEA, 38054 Grenoble cedex 09, France
[b] UMR5626, laboratoire de chimie et physique quantique, université de Toulouse, 118, route de Narbonne, 31062 Toulouse cedex, France

ABSTRACT

The electronic structure of various complexes of pentavalent uranyl species, namely UO_2^+, is described, using DFT methods, with the aim of understanding how the structure of the ligands may influence the localisation of the unpaired 5f electron of uranium (V) and, finally, the stability of such complexes towards oxidation. Six complexes have been inspected: $[UO_2py_5]^+$ (**1**), $[(UO_2py_5)KI_2]$ (**2**), $[UO_2(salan-^tBu_2)(py)K]$ (**3**), $[UO_2(salophen-^tBu_2)(thf)K]$ (**4**), $[UO_2(salen-^tBu_2)(py)K]$ (**5**), [and UO_2-cyclo[6]pyrrole]$^{1-}$ (**6**), chosen to explore various ligands. In the five first complexes, the UO_2^+ species is well identified with the unpaired electron localized on the 5f uranium orbital. Additionally, for the salan, salen and salophen ligands, some covalent interactions have been observed, resulting from the presence of both donor and acceptor binding sites. In contrast, the last complex is best described by a UO_2^{2+} uranyl (VI) coordinated by the anionic radical cyclopyrrole, the highly delocalized π orbitals set stabilizing the radical behaviour of this ligand.

© 2010 Académie des sciences. Published by Elsevier Masson SAS. All rights reserved.

1. Introduction

The description of the electronic structure of molecules containing f-elements is essential for the understanding of their chemical and physical properties and thus for the development of applications in many technological fields, such as catalysis, materials, contrast agents for magnetic resonance imaging, or the nuclear industry [1–7]. In relation to this last application, the chemistry of pentavalent uranyl has important environmental implications. Notably, the UO_2^+ species has been identified as a key intermediate in the anaerobic bacterial [8,9] or mineral mediated [10] reduction of highly soluble hexavalent uranyl species to insoluble U(IV) compounds. Since this process reduces the mobility of uranium in the environment, it is highly relevant for the speciation of uranium in the environment and for the development of remediation strategies [11].

Due to their low stability, compounds of pentavalent uranyl remain rare and only in the last few years some isolable systems have been reported. It was well known that pentavalent uranyl can be stabilized in concentrated carbonate media [12–14], but otherwise it readily disproportionates to U(IV) and uranyl(VI) species [15]. For that reason, the synthesis and isolation of stable pentavalent uranyl compounds have been a challenging task. After a first report of the crystal structure of a serendipitously-obtained cationic complex ($[UO_2(OPPh_3)_4]^+$) [16], only in the last three years have several complexes of pentavalent uranyl been reproducibly synthesized using different synthetic procedures [17,18]. However, while some complexes are fully stable, others show a limited solution stability and undergo disproportionation. The understanding of factors governing the stability of such U(V) molecular complexes is thus a crucial point. We will present here an overview of our recent theoretical advances in this challenging area.

Some efforts on theoretical grounds have been devoted since these last years to these remarkable species, in order to better understand their electronic properties but mainly

* Corresponding author. INAC/SCIB, CEA-Grenoble, 38054 Grenoble cedex 9, France.
E-mail address: pascale.maldivi@cea.fr (P. Maldivi).

on small model species [19–21]. With this aim, in a previous combined experimental and theoretical DF study [22], we have seen that depending on the chosen ligand, the unpaired f^1 electron could be completely localized on uranium or involved in a mixed f-π delocalized orbital. This latter case was observed in complexes such as the $[UO_2(salan-^tBu_2)(py)K]$ (H$_2$salan-$^tBu_2$=N,N'-bis(2-hydro-xybenzyl-3,5-ditertbutyl)-1,2-dimethylaminomethane) and $[UO_2(salophen-^tBu_2)(thf)K]$ [22]. (H$_2$salophen-$^tBu_2$= N,N'-phenylene-bis-(3,5-di-*tert*-butylsalicylideneimine) that proved to be very stable in pyridine solution. The effect being quite novel for U(V) species, we thought interesting to analyze other structures containining π-acceptor ligands that could allow a similar interaction. For instance, one of us (M.M.) has recently synthesised and structurally characterised a stable tetrameric compound of pentavalent uranyl containing the ligand salen^{2-} (H$_2$sale-n=N,N'-Bis(salicylidene)-ethylene-diamine) [23]. Such a ligand being a Schiff base as the salophen, we thought interesting to develop an electronic structure analysis in order to rationnalize these observations. Moreover, recently, Sessler et al. have synthesized the uranyl (VI) complex of a polydentate macrocycle, the cyclo[6]pyrrole [24], and they have discussed the possible formation of the analogue uranyl (V) complex in solution via electrochemi-cal reduction of the U(VI) species. We were interested thus in studying also the localization of the charge in such highly π-delocalised systems where the π* orbitals are expected to be low in energy.

Thus, we present here a comparative study of six uranyl (V) complexes which chemical properties have been already experimentally investigated as above-mentioned:

$[UO_2py_5]^+$, $[(UO_2py_5)KI_2]$, $[UO_2(salan-^tBu_2)(py)K]$, $[UO_2(salophen-^tBu_2)(thf)K]$, $[UO_2(salen-^tBu_2)(py)K]$ and $[UO_2-cyclo[6]pyrrole]^{1-}$. The formulas of the complexes are summarized on Fig. 1 as well as their numbering used throughout the study.

Complex 2 is neutral compared to complex 1, due to the addition of the KI$_2^-$ moiety as present in the crystallo-graphic structure [25]. In our previous study [22], the overall positive charge of $[UO_2py_5]^+$ was suggested to stabilize the unpaired electron in a 5f orbital. The comparison of these complexes should give a better picture of this charge effect. Complex 6 represents the possible U(V) structure obtained by Sessler et al. [24] by reduction of the isolated uranyl(VI) complex of the oxidized cyclo[6]pyrrole. This panel of complexes gives us the opportunity to study the unpaired electron localization and the stabilization of the resulting species, as a function of the ligand structure and of the total charge of the complex. As above-mentioned, some preliminary theoretical results on complexes 1, 3 and 4 were already published [22], so this present study will complete and finally give a more broad overview of the electronic and structural factors able to stabilise the U(V) state.

2. Computational methods

DFT calculations have been performed with the ADF07 package [26–28], using the PBE functional [29] built on the LDA functional of Vosko et al. [30] in an unrestricted scheme and imposing a $S=$ spin state due to the electron configuration of U(V), i.e. 5f^1. The valence space, described by a Slater type basis set (of triple-ζ quality), includes 6 s,
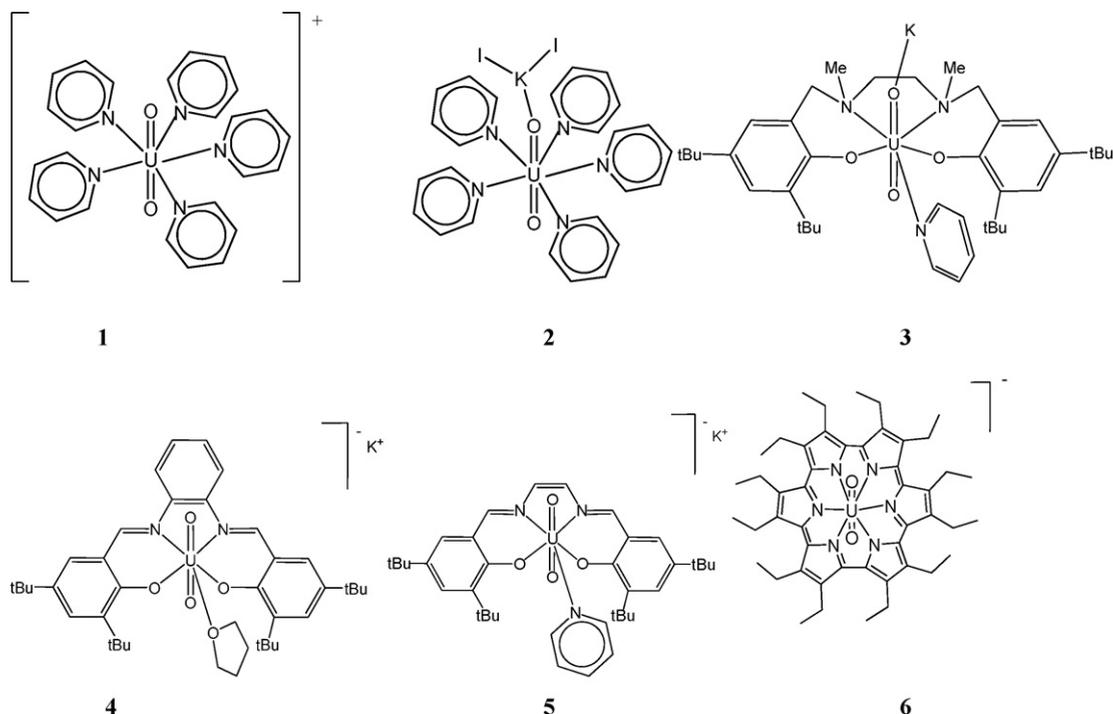
Fig. 1. Structures of the six complexes: complex 1: $[UO_2py_5]^+$; complex 2: $[(UO_2py_5)KI_2]$; complex 3: $[UO_2(salan-^tBu_2)(py)K]$; complex 4: $[UO_2(salophen-^tBu_2)(thf)K]$; complex 5: $[UO_2(salen-^tBu_2)(py)K]$; complex 6: $[UO_2-cyclo[6]pyrrole]^-$.

6p, 6d, 5f, 7 s, and a 7p polarization orbital for U, 2 s, 2p, and a 3d polarization orbital for N, C and O (triple-ζ basis sets). Core densities have been calculated for each atom by a Dirac-Slater 4-component method using the Dirac utility in ADF. The ZORA relativistic Hamiltonian [31] has been used to describe the valence density, in the scalar formalism (PBE/ZORA).

All structures have been fully optimized using tighter criteria than the standard ones. The convergence criteria were fixed to 10^{-6} Hartree and 10^{-5} Hartree/Å, respectively for the energy and the gradient and 0.1 degree for angles. The adjustable parameter which controls the precision of integrals and the mesh size for the numerical calculation of integrals has been augmented to 6.

The electronic convergence of these uranyl (V) species was difficult in some cases, due to the quasi-degeneracy of the two highest occupied Kohn-Sham orbitals. This is not related to the choice of the fonctional – as we checked by using other functionals – but is a common problem for f element chemistry because of the weakness of the ligand field. One could suggest that, in such case of near degeneracy, only multiconfigurational calculation could give a realistic description of such states. Such non-symmetric systems being too complex for a multiconfigurational calculation (see below in the discussion), we allowed fractional occupation of the Highest Occupied Molecular Orbitals (HOMOs). Thus, for these cases, a weak smear parameter was applied (0.002 Hartree) to converge, and the unpaired electron was finally localized with equal weights in two HOMOs (see below in the results part) that we will call "degenerate HOMOs". We have also tested the possibility to force a single HOMO occupation (by restarting calculation from this "smeared" density), nevertheless the total energy does not vary significantly (variation of 10^{-4} Hartree) and such solution with one electron in a HOMO with a LUMO at almost the same energy seems to us less physical that to allow a half/half electron occupation of both.

Solvent effects have been computed using a dielectric medium via the COSMO routine implemented in the ADF code. It should be stressed that in some of our systems, an explicit solvent molecule (pyridine or THF) is taken into account: for each structure, solvent molecules that were already present in the crystal have been treated explicitly. Then the continuum medium was taken as pyridine for structures from **1** to **5**, and dichloromethane for **6**, following the experimental conditions of synthesis and characterizations. Both solvents were modelled using the standard COSMO parameters.

For the five complexes **1** to **5**, where the U(V) uranyl species is present, we have estimated the stabilization energy due to coordination, through the energetic analysis of the coordination process:
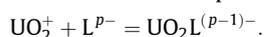
$$UO_2^+ + L^{p-} = UO_2L^{(p-1)-}.$$

L was taken as $[pyridine]_5$ ($p = 0$), $[py_5KI_2]^-$, $[Salophen-(thf)K]^-$ $[Salan-(py)K]^-$ or $[Salen-(py)K]^-$ ($p = 1$) in the structures of the final complexes. This coordination energy noted E_{coord} was calculated as E $(UO_2L^{(p-1)-})$ – $E(UO_2^+)$ – E (L^{p-}). Because UO_2^+ is open shell, it was not possible to obtain this energy in one strike using the fragment

approach of ADF, but it was necessary to calculate the three terms: E $(UO_2L^{(p-1)-})$, $E(UO_2^+)$ and E (L^{p-}). This energy must be considered only as an estimate of the interaction between the uranyl and ligands, as the latter fragments were taken in the structures of the complex.

The orbital visualization has been obtained using the graphical interface ADFGUI from ADF [32], from the species calculated in solvent.

3. Results

3.1. Geometry optimizations

The main structural parameters of the optimized structures of complexes **1**, **3**, **4**, **5**, and **6** in gas phase and in solvent (pyridine for **1** to **5** and dichloromethane for **6**) are reported in Table 1. It should be noticed that the optimized parameters in gas phase and in solvent are very close, and they are in very good agreement with experimentally available values for complexes **1**, **3**, **4**, **5**.

Some comments deserve to be added on such structural parameters. First of all, our optimized structures of complexes **3**–**5** have no symmetry because of the presence of a K^+ ion coordinated on one side of the uranyl unit. For that reason, two different distances have been reported both for the uranyl and for the U–L distances. In all complexes, the uranyl U–O bond length is slightly increased in respect to the free ion, and not perfectly linear with O–U–O angles going from 179.5 to 178.0° whereas the UO_2^+ species is linear (gas and solvent). Thus, deviations from linearity appear when equatorial ligands are present, presumably due to the non-symmetric equatorial crystal field. Another interesting feature is that for complexes **3** and **5**, the U–L(py) distance is significantly longer in the salen (2.63 Å) than in the salan (2.57 Å) species.

Then for the cyclo[6]pyrrole uranyl(V) complex **6**, no crystallographic structures are available. We can only notice that the uranyl parameters correspond rather to a U(VI) species with a short U–O bond (1.78 Å) and a linear OUO species. In fact, our parameters are very close to those found in the U(VI) homologue X-ray structure reported by Sessler in their study (U–O: 1.77 Å, U–N = 2.535 Å). We will discuss this point below in relation with the bonding analysis.

Finally, we observe only weak evolutions in the optimized distances from gas phase to solvent, but in all cases a very good agreement with experimental data. The discrepancies between gas phase and solvent are much more significant when examining interaction energies, as we will see later on, which is quite coherent because charged species are considered.

3.2. Electronic structure of the complexes

In order to study the localization of the unpaired electron, we have then inspected in detail the Kohn-Sham orbital diagrams and the nature of the HOMO or "degenerate HOMOs". In order to use familiar terms, the Kohn-Sham orbitals will be named as MOs and HOMO throughout the description.

Table 1
Geometrical parameters optimized at the PBE/TZP level of theory with pyridine as solvent (distances in Å, angles in degrees).

	U–O$_{2u}$	U–O$_{1u}$	O$_{2u}$–U–O$_{1u}$	U–O$_1$	U–O$_2$	U–N$_{1-2}$	U–S
UO$_2$$^{+a}$							
Gas	1.77		180.0				
Pyridine	1.80		179.5				
[UO$_2$py$_5$]$^{+a}$							
Gas	1.83	1.83	179.4				2.61
Pyridine	1.84	1.84	179.7				2.61
	(1.839)	*(1.839)*					*(2.614)*
[UO$_2$(salan-^{t}Bu$_2$)(py)K]^a							
Gas	1.83	1.89	177.4	2.24	2.40	2.74	2.56
Pyridine	1.83	1.89	178.0	2.25 *(2.351)*	2.39 *(2.351)*	2.74 *(2.698)*	2.57 *(2.618)*
	(1.825)		*(178.9)*				
[UO$_2$(salophen-^{t}Bu$_2$)(thf)K]							
Gas	1.81	1.86	178.3	2.31	2.33	2.58	2.64
Pyridine	1.84	1.87	178.7	2.30	2.32	2.58	2.57
	(1.851)			*(2.39)*		*(2.586)*	*(2.567)*
[UO$_2$(salen-^{t}Bu$_2$)(py)K]							
Gas	1.83	1.89	178.2	2.29	2.40	2.55	2.66
Pyridine	1.85	1.88	178.0	2.29	2.36	2.59	2.66

	U–O		O$_{2u}$–U–O$_{1u}$	U–N			
[UO$_2$-cyclo[6]pyrrole]$^{1-}$							
Gas	1.76		180.0	2.56			
Pyridine	1.78		180.0	2.53			

In italic, experimental mean distances. O$_{1u}$ and O$_{2u}$ are the uranyl oxygens; O$_1$ and O$_2$ are the phenolate oxygens and N$_{1,2}$ the donor nitrogens of salan, salen and salophen ligands. S represents a coordinated solvent: N(pyridine) for the three complexes containing pyridine, or O(THF) for the salophen complex. For the cyclo[6]pyrrole ligand, the mean U–N and U–O distances are indicated.

^{a} See Nocton et al. [22].

3.2.1. Electronic structure of complexes 1 and 2

The MO diagram for both complexes **1** and **2**, i.e. the cationic [UO$_2$py$_5$]$^+$ structure and the neutral one are shown in Fig. 2.

The 5-pyridine ligand set is not charged and the uranyl valence orbitals are too high in energy to mix with any orbital of the ligand. In particular, the unpaired alpha electron issuing from the U(V) (5f^1) electron doublet configuration is described by an almost degenerate set of two HOMOs being each occupied by half an electron, at −5.8 eV. They are pure f orbitals, one being of δ-type and the other of φ-type, by reference to the labels in uranyl linear symmetry. Moreover, the first π* orbital localized on the pyridine is at around 1 eV in respect to the HOMOs.

So for this complex, we can conclude that the electronic structure of the [UO$_2$py$_5$]$^+$ cation arises essentially from an electrostatic interaction between the pyridine ligands and the UO$_2$$^+$ cation. This is corroborated by the energy decomposition analysis provided in the next part. For the neutral complex **2** degenerate HOMOs are also obtained at a higher energy, −2.97 eV, but still strongly bound (i.e. their energy is negative), and purely localized on 5f uranium orbitals. The first lowest π* orbital is at −2 eV, so *ca.* 1 eV higher than the uranium HOMOs.

3.2.2. Complexes 3, 4 and 5

The electronic structures of the complexes [UO$_2$(salan-^{t}Bu$_2$)(py)K], [UO$_2$(salophen-^{t}Bu$_2$)(thf)K] and [UO$_2$(salen-^{t}Bu$_2$)(py)K] give rise to a different MO diagram (Fig. 3).

All the ligand sets: [(salan)(py)] [(salophen)(thf)] and [(salen)(py)] are dianionic (two negative charges located on the O phenolate) so their valence orbitals are higher in energy respect to the previous neutral 5-pyridine MOs.

The HOMOs energy level is higher for complex **3** (−2 eV) than for complexes **4** and **5**, which are almost at the same energy (*ca.* −3.1 eV). This is consistent with the higher redox potential of the U(V)/U(VI) complexes, measured for the salophen-^{t}Bu$_2$$^{2-}$ (−1.65 V vs. Fc$^+$/Fc) complex with respect to the salan-^{t}Bu$_2$$^{2-}$ one (−1.74 V vs. Fc$^+$/Fc) and with the similar redox potential measured (vs. Fc$^+$/Fc) for both the salen and salophen systems: −1.65 V (salophen) and −1.67 V (salen) [22]. For complex **3**, the degenerate set of two HOMOs is made up of two 5f orbital (δ and π type), each being combined with 35–40% of a symmetry-adapted π* orbital from the pyridine solvent coordinated. For complex **4**, the HOMO describing the unpaired alpha electron is no longer degenerate and is a combination of 47% f(δ) orbital on U and a π* orbital on the N=C Schiff base of the salophen ligand. The behaviour is similar for complex **5** with a combination of 35% f(δ) orbital on U and a π* orbital on the N=C Schiff base of the salen ligand.

3.2.3. Complex 6

The MO of the [UO$_2$-cyclo[6]pyrrole]$^{1-}$ complex is represented on Fig. 4.

The HOMO containing the unpaired alpha electron is now a π* orbital of the [cyclo[6]pyrrole]$^{2-}$ ligand, at *ca.* −3.54 eV, thus still strongly bound. The first empty alpha MO (LUMO) is indeed an f(φ) uranium orbital, located 1 eV higher in energy (Fig. 4). So, in that case, a complete transfer of the unpaired electron from the pentavalent uranyl to the ligand has taken place. The system thus formally corresponds to a uranyl(VI)- radical anion [cyclo[6]pyrrole]$^{2-•}$ structure. In spite of the 2− charge, it seems from our calculation that the π/π* MO sets of the
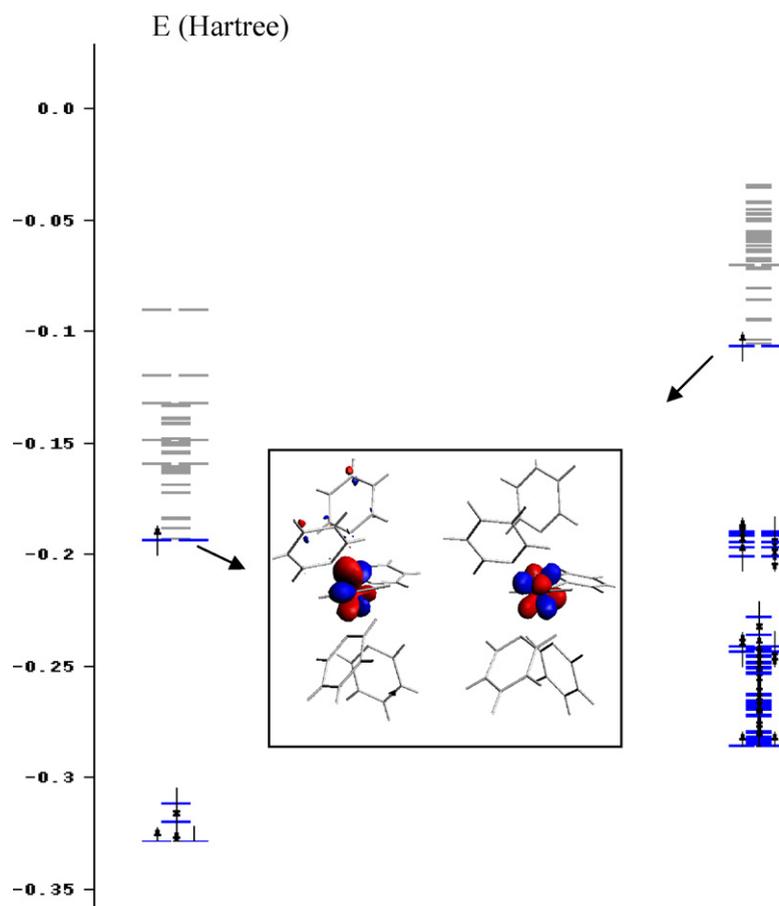
Fig. 2. MO diagram of the complexes [UO$_2$py$_5$]$^+$ (left) and [(UO$_2$py$_5$)KI$_2$] (right). The energy scale is in Hartree. The HOMOs are illustrated in the insert close to the HOMOs levels.

[cyclo[6]pyrrole]$^{2-\bullet}$ radical ligand is too low in energy respect the uranyl MO levels to lead to any covalent effect. Indeed, the uranyl distance that we obtain is 0.5 Å shorter than the 1.83–1.84 Å values observed for all the other pentavalent uranyl complexes: such distance range of 1.76–1.78 Å is characteristic of an uranyl (VI) complex.

4. Discussion

Among the six complexes studied here, we can observe different behaviours. For complexes **1** and **2**, the unpaired electron is strongly bound and localized in a 5f U orbital, whereas for complexes **3** to **5**, the unpaired electron is localised in a MO with a contribution of a 5f (U) orbital and a π* orbital of one ligand (either of the Schiff base in **4** and **5**, or of the pyridine in **3**). Finally, complex **6** is best described as a U(VI) uranyl species coordinated by the radical anionic macrocycle.

For complexes **1** to **5** where a U(V) uranyl is identified, it is interesting to analyse further the influence of the ligand structure on the bonding features. In the case of complexes **1** and **2**, the unpaired electron is in a pure 5f orbital (HOMO), the only difference being that its energy level is lower for the cationic complex **1** (−5.8 eV) than for the

neutral complex **2** (−3.0 eV). In fact, the π* levels of pyridine are too high in energy and preclude any electron transfer from U(V) to pyridine that would yield an oxidation of the uranyl moiety. It seems that even if some negative charge is present in the second sphere in complex **2**, it does not influence much the orbital levels apart from a upshift of almost 3 eV.

Complexes **3** to **5** exhibit very interesting bonding evolution with the structure of the ligand. Their common feature is the presence of two strong donor phenolate oxygens, while they differ by different types of coordinated N atoms. In the salan species, they are tertiary amines, that act only as donor atoms, thus some backbonding occurs from U(5f^1) on the pyridine ligand. In the salen and salophen species, the N coordinated sites are Schiff base functions with C=N groups, able to act as π-acceptors and the backbonding from 5f^1(U) occurs only on these groups, even when the pyridine ligand is still present as for the salen. This backbonding behaviour may be compared to the U–N distances. In Table 1, we observe that the U–S (S = py) distance is shorter with salan (2.57 Å) than with salen (2.63 Å), consistent with some backbonding on pyridine in the former, which is absent in the latter.
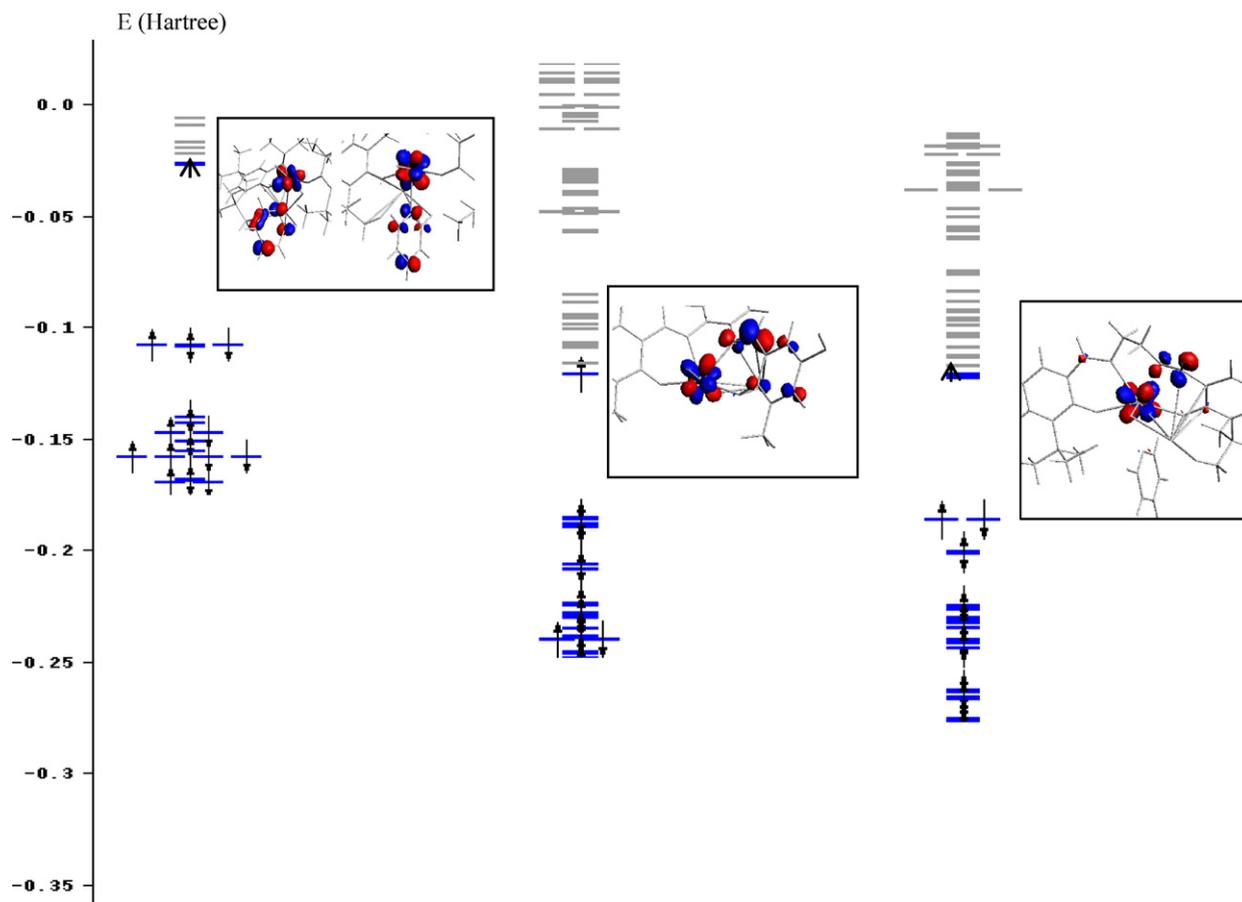
Fig. 3. MO diagrams of the complexes [UO$_2$(salan-^{t}Bu$_2$)(py)K] (left), [UO$_2$(salophen-Me$_2$)(thf)K] (middle) and [UO$_2$(salen-Me$_2$)(py)K] (right). The energy scale is in Hartree. The HOMOs are illustrated in the insert close to the HOMOs levels.

In order to better relate these bonding features to complexation interactions, we have collected in Table 2 the E$_{coord}$ (as defined in the computational details) calculated for the species in gas phase and in pyridine solvent. For this latter case, we have also indicated the energy decomposition in Pauli repulsion, Electrostatic and Orbital Interactions as provided in ADF [33,34] in order to estimate for each system the energetic contributions of electrostatic interaction and orbital relaxation.

The gas phase values of E$_{coord}$ clearly show that the two [pyridine]$_5$ complexes are less stabilized than the three salen derivatives, with E$_{coord}$ that are almost doubled for the latter (*ca.* −16 eV) compared to the former (E$_{coord}$ *ca.* −8 eV). Now, looking at the solvent calculations, we observe qualitatively the same trend in E$_{coord}$, but the discrepancy between both families of complexes has been attenuated compared to gas phase. Close examination of the various energetic contributions to this E$_{coord}$ term among the five complexes brings us more insight into the interactions put at stake in the coordination process. First of all, one main reason for the "smoothing" of E$_{coord}$ values compared to gas phase is the solvation term, i.e. the net balance between the solvation of each fragment (UO$_2^+$ and ligand) and that of the final complex. For all complexes, this balance is positive, i.e. the solvation of the complex is disfavored compared to the solvation of both individual fragments. This may be explained quite easily for the four complexes with a negative set of ligands (**2** to **5**) as both initial species (ligands and UO$_2^+$) are charged whereas the final complex is neutral. For the cationic complex **1** with five pyridines, the resulting solvation balance corresponds to only one initial species charged whereas the final complex is also charged. In that case, the solvation is still positive but smaller than for the four other ones.

Apart from this solvation term, the other energetic contributions bring to us some interesting features of the bonding. The electrostatic interaction does not vary much between all the complexes. Yet it is less negative for the cationic complex with 5-pyridine ligands (*ca.* −13 eV) than for the four others (*ca.* −14 to −16 eV). This is quite consistent with the initial species charges: in the former the interaction is between a cationic moietie (uranyle) and a neutral set of pyridines, whereas in the latter, the interaction involves a cationic uranyle with a negative set of ligands. Then the orbital energy term enlights clearly the difference of interaction between the various complexes. The three salan, salen and salophen complexes exhibit a strong negative orbital term (in a range −46 to −47.6 eV) whereas for both 5-pyridine complexes it is between −38 and −41 eV. Thus, the use of a salen-type of ligand brings a
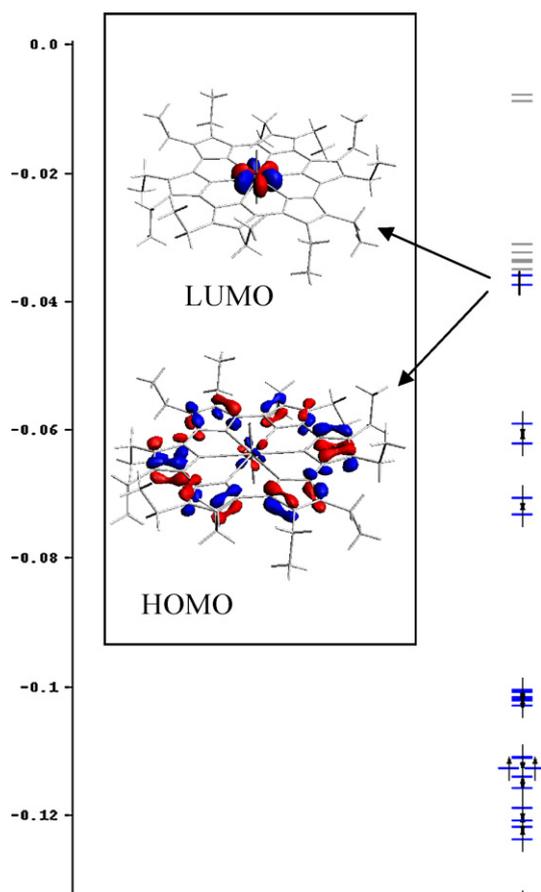
Fig. 4. MO diagrams of the complex [UO$_2$-cyclo[6]pyrrole]$^{1-}$. The energy scale is in Hartree. The HOMO and LUMO of alpha type are illustrated in the inserts.

stabilization by orbital interactions of at least –5 eV compared to the 5-pyridine ligand set. We must nevertheless remember that the orbital energy estimated within ADF corresponds to the energy change associated to the SCF process, i.e. it includes mutual polarization effects as well as covalent effects, so we must not overinterpret this term.

Nevertheless, the main conclusions of the energetic decomposition analysis is that the three salen-type ligands give uranyle (V) complexes more stabilized than with only pyridine ligands, and that the main driving force for this stabilization is due to the orbital contribution.

As mentioned when analysing the MOs, this effect may be related to the combination of both interactions – π

donation from the phenolate oxygen atoms and π-back-bonding interaction with the C=N double bonds – localized on the same ligand. This is also in agreement with the observed stability of the salophen and salen complex in all solvents and with higher resistance to hydrolysis [22,23]. These ligands seem thus to offer a synergistic effect combining highly donor phenolate groups and C=N groups acting as π-acceptor sites. This effect allows to localize the unpaired electron on uranium, thus keeping its U(V) state, and to stabilize the complexes through some covalent interactions.

Finally in the complex **6**, we observe that the unpaired electron is transferred on the π* orbital of the macrocycle, leading formally to an oxidation of the uranyl moiety and a reduction of the ligand to yield the radical anion. As above-mentioned the optimized U–N distance in complex 6 (2.53 Å, Table 1) is indeed very close to the distance found in their uranyl (VI) crystallographic structure [24]. This electron transfer is due to the highly conjugated nature of such macrocycle, which stabilizes strongly reduced ligand states. This high electronic conjugation of the cyclo[6]-pyrrole had been underlined by Sessler et al. in relation with the high planarity of the macrocycle in the uranyl (VI) species [24]. Experimentally, the nature of the radical in the one-electron reduced species – which could not be isolated – had been probed in solution through spectro-electrochemical characterizations, but could not be un-ambiguously assigned.

Finally, we should mention that the study of such large systems does not allow for multiconfigurational theoretical approaches such as the Complete Active Space (CAS) because as we can see, the uranyle–ligand interactions involve many orbitals from the uranyle and the ligands thus imply a very large active space including the 5f^1 electron and valence electrons from the ligands. This limits us to a monodeterminantal DFT study, whose reliability relies on previous numerous literature studies. From our experience on comparative DFT/CAS studies on other model systems F$_n$U–CO where n = 3, 4 or 5 with varying oxidation state of U (III, IV and V, respectively) [35], the metal-ligand interaction, charge transfer and MO description is well described by a PBE functional. We also compared various population analyses – including topological approaches – on model uranium complexes and concluded that they all gave the same trends [36]. More generally, numerous theoretical studies in the literature [37–39] on molecular uranium species show a high consistency with experimental clues in the description of the uranium-ligand bonding. Obviously, multiconfigurational studies could be undertaken but after designing

Table 2
Coordination energies (eV) E$_{coord}$ = E (UO$_2$L$^{(p-1)-}$) – E(UO$_2^+$) – E (L^{p-}) for complexes 1 to 5 (see text for details).

L	[pyridine]$_5$	[py$_5$KI$_2$]$^-$	[Salan-(py)K]$^-$	[Salen-(py)K]$^-$	[Salophen-(thf)K]$^-$
E$_{coord}$ gas	–8.37	–8.09	–14.95	–16.15	–15.7
E$_{coord}$ pyridine	–6.45	–5.29	–12.86	–8.18	–7.51
Electrostatic	–13.31	–14.38	–14.18	–15.85	–16.21
Orbital	–38.13	–41.34	–47.60	–47.20	–46.11
Solvation	3.83	5.89	5.02	7.23	7.49

All energies were calculated from the structures in the final complexes, in gas phase and pyridine solvent (COSMO). The Electrostatic and Orbital energetic contributions as given in the decomposition pathway in ADF [26] are mentioned as well as the total solvation energy.

consistent chemical models, which is out of the scope of the present manuscript.

5. Conclusion

The DFT study presented here offers the opportunity to observe different electronic behaviours of U(V) uranyl complexes, which are strongly related to the nature of the ligands. We have been able to describe complexes where the unpaired electron is clearly localized on the UO_2^+ species as in complexes **1** and **2**, complexes where some backbonding interaction with the ligand is present as in the salen and salophen compounds **4** and **5**, and finally a complex where a complete electron transfer to the ligand occurs as observed for the cyclo[6]pyrrole macrocycle. This latter behaviour may be considered as the limiting case where the backbonding from U(V) to the ligand is total. We have been able to correlate the electronic features to structural or eletrochemical behaviours when available, and more generally to known chemical properties of the various ligands. Finally, clearly a very careful match between the frontier orbitals of the ligands and of the U(V) uranyl moiety is desirable in order to be able to stabilize such pentavalent uraniums sytems. These observations pave the way for the future design of still more adapted ligands for uranyl species and exploration of their chemical properties.

References

[1] E. Ansoborlo, O. Prat, P. Moisy, C. Den Auwer, P. Guilbaud, M. Carriere, B. Gouget, J. Duffield, D. Doizi, T. Vercouter, Biochim. 88 (2006) 1605.
[2] S.A. Cotton (Ed.), Lanthanide and Actinide Chemistry, John Wiley & Sons, West Sussex, England, 2006.
[3] M.A. Denecke, P.J. Panak, F. Burdet, M. Weigl, A. Geist, R. Klenze, M. Mazzanti, K. Gompper, C. R. Chim. 10 (2007) 872.
[4] N. Kaltsoyannis, P. Scott (Eds.), The f-Elements, Oxford University Press, Oxford (England), 1999.
[5] S. Mishra, Coord. Chem. Rev. 252 (2008) 1996.
[6] K.L. Nash, in: K.A.J. Gschneider, L. Eyring, G.R. Choppin, G.H. Lander (Eds.), Handbook on the Physic and Chemistry of Rare Earths, Elsevier Science B. V, 1994.
[7] Z. Szabo, T. Toraishi, V. Vallet, I. Grenthe, Coord Chem Rev 250 (2006) 784.
[8] D.R. Lovley, E.J.P. Phillips, Y.A. Gorby, E.R. Landa, Nature 350 (1991) 413.
[9] J.C. Renshaw, L.J.C. Butchins, F.R. Livens, I. May, J.M. Charnock, J.R.E.S.T. Lloyd, Environ. Sci. Technol. 39 (2005) 5657.
[10] E.S. Ilton, A. Haiduc, C.L. Cahill, A.R. Felmy, Inorg. Chem. 44 (2005) 2986.
[11] D.E. Morris, Inorg. Chem. 41 (2002) 3542.
[12] D.L. Clark, D.E. Hobart, M.P. Neu, Chem. Rev. 95 (1995) 25.
[13] T.I. Docrat, J.F.W. Mosselmans, J.M. Charnock, M.W. Whiteley, D. Collison, F.R. Livens, C. Jones, M.J. Edmiston, Inorg. Chem. 38 (1999) 1879.
[14] A. Ikeda, C. Hennig, S. Tsushima, K. Takao, Y. Ikeda, A.C. Scheinost, G. Bernhard, Inorg. Chem. 46 (2007) 4212.
[15] L.R. Morss, N.M. Edelstein, J. Fuger (Eds.), The Chemistry of the Actinide and Transactinide Elements, Springer, Dordrecht, 2006.
[16] J.-C. Berthet, M. Nierlich, M. Ephritikhine, Angew. Chem. Int. Ed. 42 (2003) 1952.
[17] P.L. Arnold, J.B. Love, D. Patel, Coord. Chem. Rev. 253 (2009) 1973.
[18] C.R. Graves, J.L. Kiplinger, Chem. Commun. (2009) 3831.
[19] L. Gagliardi, I. Grenthe, B.O. Roos, Inorg. Chem. 40 (2001) 2976.
[20] N. Iche-Tarrat, N. Barros, C.J. Marsden, L. Maron, Chem. Eur. J. 14 (2008) 2093.
[21] F. Ruiperez, C. Danilo, F. Real, J.P. Flament, V. Vallet, U. Wahlgren, J. Phys. Chem. A 113 (2009) 1420.
[22] G. Nocton, P. Horeglad, V. Vetere, J. Pecaut, L. Dubois, P. Maldivi, N.M. Edelstein, M. Mazzanti, J. Am. Chem. Soc. (2009) ASAP.
[23] V. Mougel, P. Horeglad, G. Nocton, J. Pecaut, M. Mazzanti, Angew. Chem. Int. Ed. 48 (2009) 8477.
[24] P.J. Melfi, S.K. Kim, J.T. Lee, F. Bolze, D. Seidel, V.M. Lynch, J.M. Veauthier, A.J. Gaunt, M.P. Neu, Z. Ou, K.M. Kadish, S. Fukuzumi, K. Ohkubo, J.L. Sessler, Inorg. Chem. 46 (2007) 5143.
[25] J.C. Berthet, G. Siffredi, P. Thuery, M. Ephritikhine, Dalton Trans. (2009) 3478.
[26] ADF 2007.01, SCM, Amsterdam, The Nederlands, www.scm.com.
[27] P.M. Boerrigter, G.T. Velde, E.J. Baerends, Int. J. Quant. Chem. 33 (1988) 87.
[28] G.T. Velde, F.M. Bickelhaupt, E.J. Baerends, C.F. Guerra, S.J.A. Van Gisbergen, J.G. Snijders, T. Ziegler, J. Comput. Chem. 22 (2001) 931.
[29] J.P. Perdew, K. Burke, M. Ernzerhof, Phys. Rev. Lett. 77 (1996) 3865.
[30] S.H. Vosko, L. Wilk, M. Nusair, Can. J. Phys. 58 (1980) 1200.
[31] E. van Lenthe, R. van Leeuwen, E.J. Baerends, J.G. Snijders, Int. J. Quant. Chem. 57 (1996) 281.
[32] ADF-GUI 2007.01, SCM, Amsterdam, The Nederlands. www.scm.com.
[33] T. Ziegler, A. Rauk, Inorg. Chem. 18 (1979) 1755.
[34] T. Ziegler, A. Rauk, Inorg. Chem. 18 (1979) 1558.
[35] V. Vetere, P. Maldivi, B.O. Roos, C. Adamo, J. Phys. Chem. A 113 (2009) 14760.
[36] L. Petit, L. Joubert, P. Maldivi, C. Adamo, J. Am. Chem. Soc. 128 (2006) 2190.
[37] J.P. Hay, Faraday Discuss. 124 (2003) 69.
[38] L. Maron, O. Eisenstein, R.A. Andersen, Organometallics 28 (2009) 3629.
[39] S.A. Kozimor, P. Yang, E.R. Batista, K.S. Boland, C.J. Burns, D.L. Clark, S.D. Conradson, R.L. Martin, M.P. Wilkerson, L.E. Wolfsberg, J. Am. Chem. Soc. 131 (2009) 12125.